Petroleum Science 19 (2022) 2867–2878

Contents lists available at ScienceDirect

Petroleum Science

journal homepage: www.keaipublishing.com/en/journals/petroleum-science

Original Paper

The generalized method for estimating reserves of shale gas and coalbed methane reservoirs based on material balance equation

Jun-Tai Shi [a, b, *], Yan-Ran Jia [a, b], Long-Long Zhang [a, b], Chang-Jiang Ji [c], Guo-Fu Li [c], Xian-Yue Xiong [d], Hong-Xing Huang [e], Xiang-Fang Li [a, b], Sui-An Zhang [a, b]

[a] State Key Laboratory of Petroleum Resources and Prospecting in China University of Petroleum (Beijing), Beijing, 102249, China
[b] Coalbed Methane Research Center, China University of Petroleum (Beijing), Beijing, 102249, China
[c] State Key Laboratory of Coal and CBM Co-Mining in Nancun Town, Jincheng, 048012, Shanxi, China
[d] PetroChina Coalbed Methane Company Limited, Beijing, 100028, China
[e] China United Coalbed Methane National Engineering Research Center Co. Ltd, Beijing, 100095, China

ARTICLE INFO

Article history:
Received 2 January 2022
Received in revised form
25 July 2022
Accepted 28 July 2022
Available online 2 August 2022

Edited by Yan-Hua Sun

Keywords:
Shale gas
Coalbed methane
Material balance equation
Reserve evaluation
Dissolved gas
Generalized method

ABSTRACT

As the main unconventional natural gas reservoirs, shale gas reservoirs and coalbed methane (CBM) reservoirs belong to adsorptive gas reservoirs, i.e., gas reservoirs containing adsorbed gas. Shale gas and CBM reservoirs usually have the characteristics of rich adsorbed gas and obvious dynamic changes of porosity and permeability. A generalized material balance equation and the corresponding reserve evaluation method considering all the mechanisms for both shale gas reservoirs and CBM reservoirs are necessary. In this work, a generalized material balance equation (GMBE) considering the effects of critical desorption pressure, stress sensitivity, matrix shrinkage, water production, water influx, and solubility of natural gas in water is established. Then, by converting the GMBE to a linear relationship between two parameter groups related with known formation/fluid properties and dynamic performance data, the straight-line reserve evaluation method is proposed. By using the slope and the *y*-intercept of this straight line, the original adsorbed gas in place (OAGIP), original free gas in place (OFGIP), original dissolved gas in place (ODGIP), and the original gas in place (OGIP) can be quickly calculated. Third, two validation cases for shale gas reservoir and CBM reservoir are conducted using commercial reservoir simulator and the coalbed methane dynamic performance analysis software, respectively. Finally, two field studies in the Fuling shale gas field and the Baode CBM field are presented. Results show that the GMBE and the corresponding straight-line reserve evaluation method are rational, accurate, and effective for both shale gas reservoirs and CBM reservoirs. More detailed information about reserves of shale gas and CBM reservoirs can be clarified, and only the straight-line fitting approach is used to determine all kinds of reserves without iteration, proving that the proposed method has great advantages compared with other current methods.

1. Introduction

Shale gas and coalbed methane (CBM) are major alternatives to conventional gas resources. Due to the large amount of natural gas in adsorption state buried in CBM reservoirs and shale gas reservoirs, it brings great challenges to reserve evaluation using material balance equation (MBE) comparing with conventional gas reservoirs. Therefore, in order to evaluate the reserves of shale gas reservoirs and CBM reservoirs, the first essential step is to establish a suitable MBE for these two gas reservoirs.

CBM reservoir contains so much water that it usually goes through water drainage stage before gas desorption and production. For shale gas reservoirs, more and more studies show that the initial water saturation is usually high, such as, 25%–35% in Barnett shale and up to 40%–46% in Changning-Weiyuan shale (Akkutlu et al., 2015; Fuentes-Cruz and Vasquez-Cruz, 2022; Kazemi and Ghaedi, 2020; Li et al., 2016; Orozco and Aguilera, 2017, 2018), resulting in that the original dissolved gas in place (ODGIP) can

* Corresponding author. State Key Laboratory of Petroleum Resources and Prospecting in China University of Petroleum (Beijing), Beijing, 102249, China.
E-mail address: shijuntai@cup.edu.cn (J.-T. Shi).

https://doi.org/10.1016/j.petsci.2022.07.009

Nomenclature

A	Control area, 10^8 m^2
B_g	Gas volume factor at the current state, m^3/sm^3
B_{gi}	Initial gas volume factor, m^3/sm^3
B_w	Water volume factor at current state, m^3/sm^3
B_{wi}	Initial water volume factor, m^3/sm^3
b	y-intercept of the straight line, 10^8 m^3
c_a	Coal matrix shrinkage coefficient, dimensionless
c_p	Pore compressibility, MPa^{-1}
c_s	Dissolution coefficient of natural gas in water, MPa^{-1}
c_w	Water compressibility, MPa^{-1}
G_{ai}	Original adsorbed gas in place (OAGIP), 10^8 m^3
G_{fi}	Original free gas in place (OFGIP), 10^8 m^3
G_i	Original gas in place (OGIP), 10^8 m^3
G_p	Cumulative gas production, 10^8 m^3
G_{si}	Original dissolved gas in place (ODGIP), 10^8 m^3
H	Henry's constant, MPa
h	Formation thickness, m
m	The slope of the straight line, 10^8 m^3
p_d	Critical desorption pressure, MPa
p_i	Initial reservoir pressure, MPa
$\overline{p}$	Average formation pressure, MPa
p_L	Langmuir pressure, MPa
p_{sc}	Standard pressure, MPa
p_{wf}	Bottom-hole flowing pressure, MPa
Q_g	Gas production rate, m^3/d
Q_w	Water production rate, m^3/d
S_{wi}	Initial water saturation, fraction
T	Reservoir temperature, K
T_{sc}	Standard temperature, K
V_L	Langmuir volume, m^3/t
W_e	Water influx, 10^8 m^3
W_p	Cumulative water production, 10^8 m^3
X	The value of x axis for reserve evaluation method, dimensionless
Y	The value of y axis for reserve evaluation method, 10^8 m^3
$\overline{Z}$	Average gas deviation factor, dimensionless
Z_{sc}	Gas deviation factor at standard condition, dimensionless
ρ_B	Bulk density of rock, t/m^3
γ_g	Gas specific gravity, dimensionless
ϕ_i	Initial reservoir porosity, fraction
ν	Poisson's ratio, fraction
ε_{max}	Maximum strain of matrix shrinkage, fraction

account for more than 2.2%–6.6% of original free gas in place (OFGIP) for some cases (Zhou et al., 2013). Therefore, dissolved gas in water is essential to MBEs for CBM reservoirs and shale gas reservoirs, and ODGIP cannot be ignored during the reserve evaluation for these two gas reservoirs.

Different from the occurrence state of free gas in conventional gas reservoirs, adsorptive gas reservoirs have not only free gas, but also adsorbed gas (Ahmed et al., 2006; Clarkson and McGovern, 2001; King, 1990, 1993; Li et al., 2020; Liu et al., 2021; Moghadam et al., 2009, 2011; Nie et al., 2021; Pan et al., 2020; Seidle, 1999; Sun et al., 2021; Wang et al., 2021; Yang et al., 2021; Zhu et al., 2020) and dissolved gas (Akkutlu et al., 2015; Fuentes-Cruz and Vasquez-Cruz, 2022; Kazemi and Ghaedi, 2020; Orozco and Aguilera, 2017, 2018; Shi et al., 2018a; Zhou et al., 2013). Compared with reserve evaluation of conventional gas reservoirs (Shi et al., 2021c), the reserve evaluation of adsorptive gas reservoirs needs to consider the following three particularities: first, the desorption process in the production process of adsorptive gas reservoir needs to be considered. Only when the pressure is lower than the critical desorption pressure, the adsorbed gas begins to desorb; second, it is necessary to consider the dual effects of stress sensitivity and matrix shrinkage on porosity in the production of adsorptive gas reservoirs; third, it is necessary to consider the impact of dissolved gas overflow on gas production and pressure.

King (1990, 1993) first proposed an MBE for CBM reservoir considering gas adsorption and desorption, and then constructed a linear relationship of p/Z^* versus G_p through defining a pseudo-deviation factor Z^* to estimate the original gas in place for CBM reservoirs. King's discovery is significant, but the calculating process needs iteration, and some essential factors influencing CBM production, such as, critical desorption pressure, matrix shrinkage, and dissolved gas, were ignored. Jensen and Smith (1997) derived an MBE for CBM reservoir by only considering gas in adsorbed state, so it was simple and limited in use. Seidle (1999) simplified King's MBE by neglecting formation compressibility, water compressibility, and water influx. Seidle's discovery greatly simplified the MBE and facilitated reserve calculation process directly using inversion instead of iteration, but some essential factors influencing CBM production were still ignored. Clarkson and McGovern (2001) extended the application scope of Jensen and Smith's MBE, by considering the existence of free gas. However, in order to simplify the calculation process, it is assumed that the water saturation is constant during the CBM production process.

Ahmed et al. (2006) proposed an MBE for CBM reservoir considering free gas, water expansion, formation compressibility, and gas adsorption/desorption using Langmuir equation, and divided the MBE into two cases according to whether the compressibilities of rock and fluid were considered. Based on this MBE, reserves can be calculated directly without iteration. However, the essential factors such as the critical desorption pressure, matrix shrinkage, and dissolved gas are still not considered.

Based on King and Ahmed's MBE, Chen and Hu (2008) proposed an MBE for CBM reservoir to calculate original adsorbed gas in place (OAGIP) and original free gas in place (OFGIP). However, this MBE still neglects original dissolved gas in place and critical desorption pressure. Moghadam et al. (2009, 2011) considered formation compressibility, expansion of residual fluid, gas adsorption/desorption, and water influx into the MBE for CBM reservoirs, then in order to calculate reveres by directly inversion, they proposed a new pseudo-deviation factor Z^{**} to simplify the MBE. However, the critical desorption pressure, matrix shrinkage, and dissolved gas are still not considered.

Assuming that adsorbed gas occupies a certain amount of pore space, Williams-Kovacs et al. (2012) developed an MBE for shale gas reservoirs, in which the porosity of adsorbed gas phase was considered to be affected by pore pressure. Zhang et al. (2013) also proposed an MBE for shale gas reservoirs based on Williams-Kovacs's assumption. However, these two MBEs ignored gas solubility, water influx, and water production.

Ibrahim and Nasr-El-Din (2015) proposed an MBE for CBM reservoirs, which took into account methane solubility, matrix shrinkage, and formation compressibility. Compared with King's MBE (King, 1993), Clarkson and McGovern's MBE (Clarkson and McGovern, 2001), and their MBE without matrix shrinkage, it was

found that the original gas in place (OGIP) was underestimated roughly 10% if ignoring matrix shrinkage effect. However, the inversion plot was not strictly straight which seriously affected the accuracy of reserve calculation.

On the basis of the existence of adsorbed gas, free gas, and dissolved gas in CBM reservoirs, Shi et al. (2018a) derived an MBE and proposed a linear reserve evaluation method for CBM reservoirs using a pseudo-deviation factor Z^* incorporating pore compressibility and matrix shrinkage effects. However, the calculation process of Z^* is still complex.

From the above literature review, it can be concluded that the current material balance equations and reserve evaluation methods for shale gas reservoirs and CBM reservoirs either ignored at least one or more important mechanisms or their calculating processes were complex. In addition, the current material balance equations and reserve evaluation methods are only suitable to one type gas reservoir, the generalized reserve evaluation method based on material balance equation suitable for both shale gas reservoirs and CBM reservoirs is lacking. Hence, a comprehensive and generalized MBE and reserve evaluation method for adsorptive gas reservoirs, including shale gas reservoirs and CBM reservoirs, are necessary. In this work, first, a generalized material balance equation (GMBE) considering the critical desorption pressure, pore volume variation due to stress sensitivity and matrix shrinkage, water production, water flux, and dissolved gas in water is established. Then, a straight-line reserve evaluation method is proposed through conversion of the established GMBE. Third, the credibility of GMBE and straight-line reserve evaluation method are verified by numerical simulation of a shale gas reservoir and a CBM reservoir. Finally, the proposed straight-line reserve evaluation method is applied to the Fuling shale gas reservoir and the Baode CBM reservoir.

2. Establishments of GMBE and reserve evaluation method

2.1. Establishment of GMBE for shale gas and CBM reservoirs

For shale gas reservoirs, free gas and adsorbed gas are two main gas types. Besides, the dissolved gas should be considered in case that much water exists in shale matrix and the reservoir pressure is high. For under-saturated CBM reservoirs, the initial reservoir pressure is above the critical desorption pressure, there is a water drainage stage, most natural gas exists in adsorbed state, only small percentage of natural gas is in dissolved state. In addition, free gas may also exist in under-saturated CBM reservoirs if the reservoir is lifted to shallow stratum after gas generation. For saturated CBM reservoirs, the initial reservoir pressure is equal to or below the critical desorption pressure, at the beginning of gas production, the adsorbed gas will desorb, so the produced gas consists of desorbed gas, free gas, and dissolved gas. Thus, in order to include all the circumstance in different kinds of shale gas reservoirs and CBM reservoirs, adsorbed gas, free gas, and dissolved gas, these three gas types should be all considered when establishing the material balance equation.

According to the material balance principle, the cumulative gas production is equal to the original gas in place minus the residual gas reserve. The generalized MBE for shale gas reservoirs and CBM reservoirs can be written as:

$$G_p = Ah\frac{\rho_B V_L p_d}{p_L + p_d} + \frac{Ah\phi_i(1-S_{wi})Z_{sc}T_{sc}p_i}{p_{sc}TZ_i} + Ah\phi_i S_{wi}c_s p_i - Ah\frac{\rho_B V_L \overline{p}}{p_L + \overline{p}} - \frac{Ah\phi(1-S_w)Z_{sc}T_{sc}\overline{p}}{p_{sc}T\overline{Z}} - Ah\phi S_w c_s \overline{p} \quad (1)$$

One point that needs to explain is that, for under-saturated CMB reservoirs, during the water drainage stage, i.e., the average reservoir pressure is high than the critical desorption pressure, since the adsorbed gas hasn't desorbed, the term for adsorbed gas should be ignored.

During the shale gas and CBM production, the reservoir porosity will change owing to stress sensitivity and matrix shrinkage effects. Stress sensitivity occurring during the whole production decreases porosity. However, the matrix shrinkage effect increases porosity after the adsorbed gas starts to desorb (Harpalani and Schraufnagel, 1990; Miao et al., 2020, 2022). The porosity model considering both effects of stress sensitivity and matrix shrinkage (Clarkson et al., 2010; Liu and Harpalani, 2013; Palmer, 2009; Shi and Durucan, 2005) can be expressed as:

$$\phi = \phi_i\left[1 - c_p(p_i - \overline{p}) + c_a\left(\frac{p_d}{p_L + p_d} - \frac{\overline{p}}{p_L + \overline{p}}\right)\right] \quad (2)$$

where ϕ is the current reservoir porosity; c_a is the matrix shrinkage coefficient, dimensionless. According to the experimental results from Ibrahim and Nasr-El-Din (2015), the value of c_a varies from 0.002 to 0.026. The definition of c_a is:

$$c_a = \frac{2\nu\varepsilon_{max}}{1+2\nu} \quad (3)$$

where ε_{max} is the maximum adsorption/desorption volume strain of matrix, which is generally not more than 0.1; ν is Poisson's ratio.

In order to incorporate the effect of dissolved gas into MBE, the dissolution coefficient of natural gas in water c_s is introduced, which can be calculated by:

$$c_s = \frac{22.4}{0.018H} \quad (4)$$

where H is Henry's constant, MPa.

In addition, the underground volume of the produced water is equal to the volume of the original water minus the volume occupied by the current water and then plus the volume of water expansion and the volume of water influx. Then the material balance equation of water phase can be expressed as:

$$W_p B_w = Ah\phi_i S_{wi} - Ah\phi S_w + Ah\phi_i S_{wi} c_w(p_i - \overline{p}) + W_e \quad (5)$$

Substituting Eq. (2) into Eq. (5) yields:

$$S_w = \frac{S_{wi}[1 + c_w(p_i - \overline{p})] + \frac{W_e - W_p B_w}{Ah\varphi_i}}{1 - c_p(p_i - \overline{p}) + c_a\left(\frac{p_d}{p_L + p_d} - \frac{\overline{p}}{p_L + \overline{p}}\right)} \quad (6)$$

It is assumed that temperature T, initial porosity ϕ_i, Langmuir constants V_L and p_L, dissolution coefficient of methane in water c_s, pore compressibility c_p, water compressibility c_w, initial water saturation S_{wi}, and water influx W_e (referred to underground volume) are known.

The term $\phi(1 - S_w)$ can be calculated using Eqs. (2) and (6), which is shown as,

$$\phi(1-S_w)=\phi_i\left[1-S_{wi}-(c_p+S_{wi}c_w)(p_i-\overline{p})-\frac{W_e-W_pB_w}{Ah\phi_i}+c_a\left(\frac{p_d}{p_L+p_d}-\frac{\overline{p}}{p_L+\overline{p}}\right)\right] \tag{7}$$

Substituting Eqs. (2), (6) and (7) into Eq. (1) gives,

$$G_p=Ah\frac{\rho_B V_L p_d}{p_L+p_d}+\frac{Ah\phi_i(1-S_{wi})Z_{sc}T_{sc}p_i}{p_{sc}TZ_i}+Ah\phi_i S_{wi}c_s p_i-Ah\frac{\rho_B V_L\overline{p}}{p_L+\overline{p}}-Ah\phi_i c_s\overline{p}\left[S_{wi}[1+c_w(p_i-\overline{p})]+\frac{W_e-W_pB_w}{Ah\phi_i}\right]-\frac{Ah\phi_i Z_{sc}T_{sc}\overline{p}}{p_{sc}T\overline{Z}}\left[1-S_{wi}-(c_p+S_{wi}c_w)(p_i-\overline{p})-\frac{W_e-W_pB_w}{Ah\phi_i}+c_a\left(\frac{p_d}{p_L+p_d}-\frac{\overline{p}}{p_L+\overline{p}}\right)\right] \tag{8}$$

Eq. (8) will be the generalized material balance equation (GMBE) for both shale gas reservoirs and CBM reservoirs.

2.2. The method for calculating OGIP of shale gas and CBM reservoirs

2.2.1. Reorganizing Eq. (8) yields

$$G_p-\left(\frac{Z_{sc}T_{sc}\overline{p}}{p_{sc}T\overline{Z}}-c_s\overline{p}\right)(W_e-W_pB_w)=\frac{Ah\phi_i(1-S_{wi})Z_{sc}T_{sc}p_i}{p_{sc}TZ_i}+Ah\left\{\frac{\rho_B V_L p_d}{p_L+p_d}-\frac{\rho_B V_L\overline{p}}{p_L+\overline{p}}-\frac{\phi_i Z_{sc}T_{sc}\overline{p}}{p_{sc}T\overline{Z}}\left[1-S_{wi}-(c_p+S_{wi}c_w)(p_i-\overline{p})+c_a\left(\frac{p_d}{p_L+p_d}-\frac{\overline{p}}{p_L+\overline{p}}\right)\right]+\phi_i S_{wi}c_s(p_i-\overline{p})(1-\overline{p}c_w)\right\} \tag{9}$$

Eq. (9) can be rewritten as:

$$Y=b+m\cdot X \tag{10}$$

with

$$Y=G_p-\left(\frac{Z_{sc}T_{sc}\overline{p}}{p_{sc}T\overline{Z}}-c_s\overline{p}\right)(W_e-W_pB_w) \tag{11}$$

$$X=\frac{\rho_B V_L p_d}{p_L+p_d}-\frac{\rho_B V_L\overline{p}}{p_L+\overline{p}}-\frac{\phi_i Z_{sc}T_{sc}\overline{p}}{p_{sc}T\overline{Z}}\left[1-S_{wi}-(c_p+S_{wi}c_w)(p_i-\overline{p})+c_a\left(\frac{p_d}{p_L+p_d}-\frac{\overline{p}}{p_L+\overline{p}}\right)\right]+\phi_i S_{wi}c_s(p_i-\overline{p})(1-\overline{p}c_w) \tag{12}$$

$$b=\frac{Ah\phi_i(1-S_{wi})Z_{sc}T_{sc}p_i}{p_{sc}TZ_i} \tag{13}$$

$$m=Ah \tag{14}$$

As shown in Eq. (10), if drawing a plot of Y versus X, a straight line with b as the y-intercept and m as the slope will be obtained. Through data fitting, the y-intercept b and the slope m can be determined.

Thus, the control volume of the reservoir Ah will be the slope of this straight line m, and the original free gas in place (OFGIP) will be the y-intercept of this straight line b.

Alternatively, the OFGIP of the reservoir can be also calculated using the slope of the straight line:

$$G_{fi}=m\frac{\phi_i(1-S_{wi})Z_{sc}T_{sc}p_i}{p_{sc}TZ_i} \tag{15}$$

Using the slope of the straight line m, the original adsorbed gas in place (OAGIP) can be easily calculated as:

$$G_{ai}=m\frac{\rho_B V_L p_d}{p_L+p_d} \tag{16}$$

The original dissolved gas in place (ODGIP) can be calculated as:

$$G_{si}=m\phi_i S_{wi}p_i c_s \tag{17}$$

Thus, the original gas in place (OGIP) for shale gas reservoir and CBM reservoir can be calculated by summation of original free gas in place, original adsorbed gas in place, and original dissolved gas in place, which is:

$$G_i=G_{ai}+G_{fi}+G_{si} \tag{18}$$

2.3. Calculation procedures

The procedure to estimate the original gas in place of shale gas reservoirs and CBM reservoirs is recommended as follows:

(1) Select the formation and fluid physical parameters of the given shale gas reservoir or CBM reservoir, including: bulk density of rock ρ_B, Langmuir volume V_L, Langmuir pressure p_L, critical desorption pressure p_d, reservoir temperature T, initial reservoir pressure p_i, initial reservoir porosity ϕ_i, initial water saturation S_{wi}, pore volume compressibility c_p, formation water compressibility c_w, formation water volume factor B_w, specific gravity of natural gas γ_g, Herry's constant H, Poisson's ratio ν, and maximum adsorption/desorption volume strain of matrix ε_{max}.

(2) Determine the values of matrix shrinkage coefficient c_a and dissolution coefficient of natural gas in water c_s. If the matrix shrinkage coefficient c_a and the dissolution coefficient of natural gas in water c_s are not available, Eq. (3) can be used to determine the matrix shrinkage coefficient c_a using Poisson's ratio ν and maximum adsorption/desorption volume strain of matrix ε_{max}, and Eq. (4) is recommended to determine the dissolution coefficient of natural gas in water c_s. If the matrix shrinkage coefficient c_a and dissolution coefficient of natural gas in water c_s are available, just straightly use them.

(3) Select the production dynamic performance data for the given shale gas reservoir or CBM reservoir, including

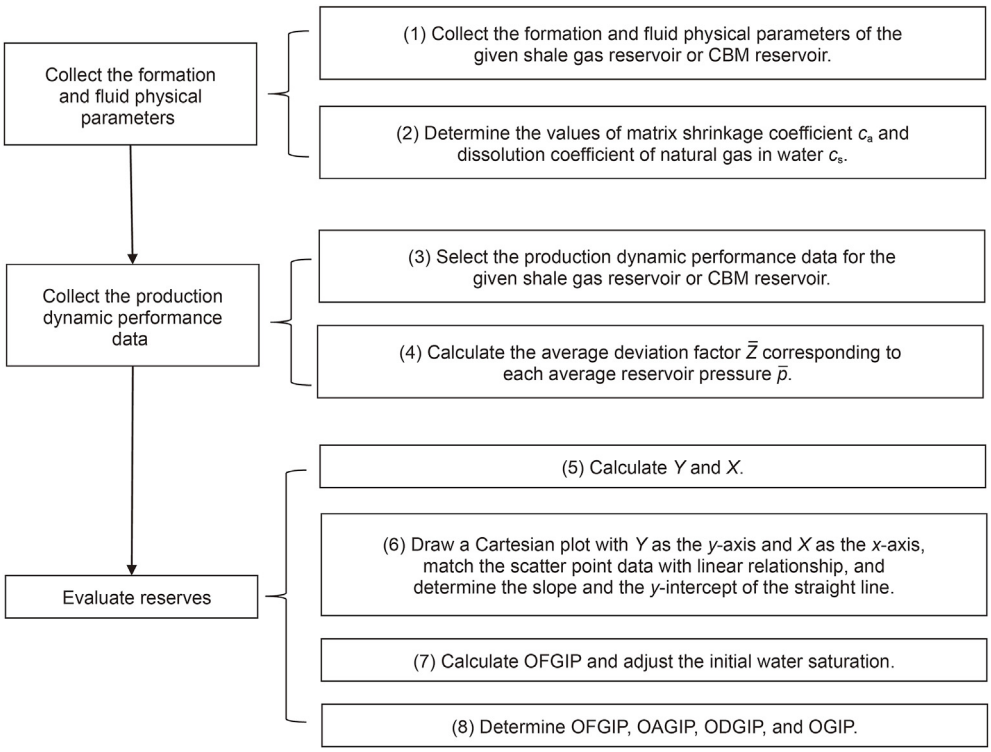

Fig. 1. Flowchart of the approach for estimating reserves of shale gas and coalbed methane reservoirs.

cumulative gas production G_p, cumulative water production W_p, average reservoir pressure $\bar{p}$, and cumulative water influx W_e (referred to underground volume) at the same production time, and at least three sets of dynamic data corresponding to different time are required. Actually, for shale gas reservoirs and CBM reservoirs, the control area is divided into many pieces by multiple production wells, and the reservoir boundary is affected and controlled by these production wells. Hence, it can be assumed that there is no edge and bottom water supply at the reservoir boundary for shale gas reservoir and CBM reservoir, i.e., cumulative water influx W_e can be set to be 0 for shale gas reservoirs and CBM reservoirs in most cases.

(4) Calculate the average deviation factor $\bar{Z}$ corresponding to each average reservoir pressure $\bar{p}$. If the average gas deviation factor $\bar{Z}$ is unknown, the Dranchuk–Abou-Kassem method (Dranchuk and Abou-Kassem, 1975) is recommended to calculate $\bar{Z}$ at any average formation pressure $\bar{p}$ based on reservoir temperature T and specific gravity of natural gas γ_g.

(5) Calculate Y and X for each production time corresponding each average reservoir pressure through substituting the formation and fluid physical parameters and production dynamic performance data into Eqs. (11) and (12), respectively.

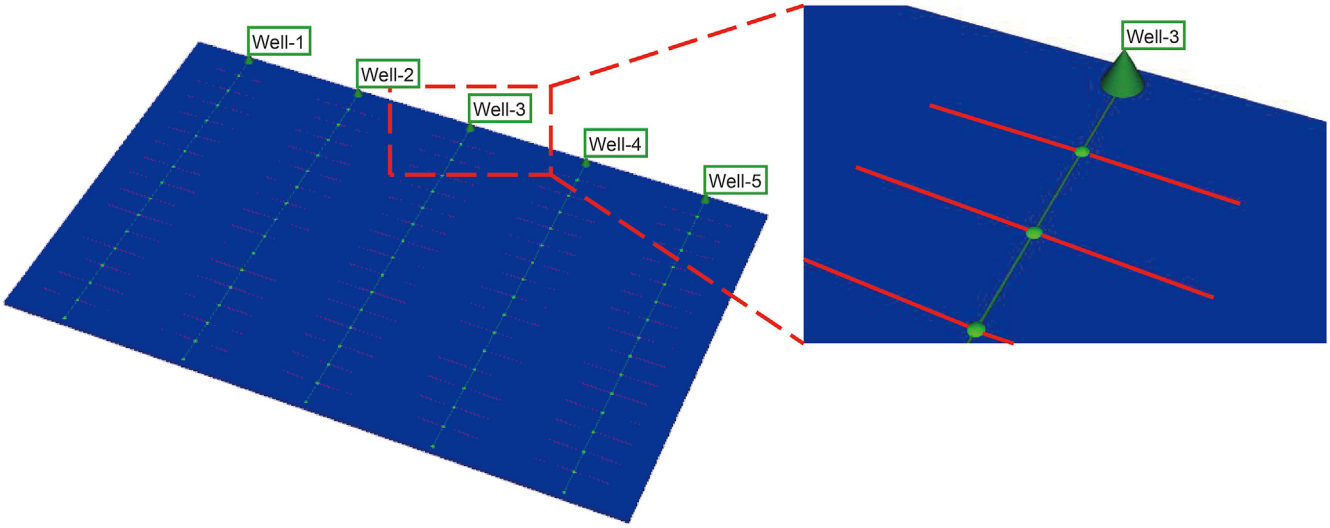

Fig. 2. Numerical simulation model of the shale gas reservoir.

Table 1
Formation and fluid properties of the shale gas reservoir.

Parameter	Value
Bulk density of rock ρ_B, t/m^3	2.5
Langmuir volume V_L, m^3/t	3.94
Langmuir pressure p_L, MPa	8
Critical desorption pressure p_d, MPa	37.69
Initial pressure p_i, MPa	37.69
Initial porosity ϕ_i	0.051
Initial water saturation S_{wi}	0.4
Pore volume compressibility c_p, MPa^{-1}	0.001
Water compressibility c_w, MPa^{-1}	0.000435
Water volume factor B_w, m^3/sm^3	1
Specific gravity of natural gas γ_g	0.56
Formation temperature T, K	355.35
Dissolution coefficient of natural gas in water c_s, MPa^{-1}	0
Matrix shrinkage coefficient c_a	0

(6) Draw a plot with Y as the y-axis and X as the x-axis, match the scatter point data with linear relationship, and determine the y-intercept b and the slope m of this straight line.
(7) Calculate OFGIP using both the y-intercept b and the slope m of the straight line, if the value calculated by the slope of this straight line and that by the y-intercept of the straight line are not the same, adjust the initial water saturation S_{wi}, repeat steps 1–7 until these two values are close.
(8) Determine OFGIP, OAGIP, ODGIP, and OGIP through substituting b and m into Eqs. (15)–(18).

The flowchart of the approach for estimating reserves of shale gas and coalbed methane reservoirs is shown as in Fig. 1.

3. Validations

3.1. Validation for shale gas reservoir

The commercial reservoir simulator, IMEX section in Computer Modelling Group (CMG-IMEX), is applied to simulate the production of a shale gas reservoir.

Fig. 2 shows the numerical simulation model for this shale gas reservoir, which is a cuboid with a length of 2628.5 m, a width of 1653.3 m, and a height of 20.1 m. The single porosity model is used, and the gas supply mechanism through desorption of adsorbed gas is considered. This assumption is reasonable and acceptable because for the material balance calculations, the measured average reservoir pressure is actually the balanced pressure in fracture system after a period of well shut-in. In addition, gas and water two-phase flow is used for the fluid model. The formation and fluid properties of this model are shown in Table 1. Output from this simulation model, the pore volume is 0.87348551×10^8 m^3, the original free gas in place (OFGIP) is 7.86364717×10^8 m^3, the original adsorbed gas in place (OAGIP) is 7.09712062×10^8 m^3, and the original gas in place (OGIP) is 14.96076779×10^8 m^3. One thing which needs to mention is that because the dissolve gas cannot be simulated in CMG, so the dissolve gas is not considered in this validation case.

Five multi-stage fractured horizontal wells are evenly arranged in the shale gas reservoir. For each well, the length of horizontal section is 1603.2 m, the number of perforated sections is 15, and the fracture half-length is 150 m. Each well is scheduled to produce gas of 50,000 m^3/d. After the bottom-hole flowing pressure drops to the minimum bottom-hole flowing pressure of 10 MPa, it remains stable. The production performance for one well is shown in Fig. 3a. The cumulative gas production G_p and cumulative water production W_p of the whole gas reservoir are shown in Fig. 3b. The average formation pressure $\bar{p}$ and the average deviation factor $\bar{Z}$ of the whole gas reservoir are shown in Fig. 3c. For simplification of the validation process, water influx, dissolved gas in water, and matrix shrinkage effect are not considered for this shale gas reservoir, i.e., the W_e value is constant at 0, the dissolution coefficient of natural gas in water c_s is 0, and the matrix shrinkage coefficient c_a is 0.

The annual production performance data of this shale gas reservoir are listed in Table 2, including date, cumulative water production W_p, cumulative gas production G_p, average formation pressure $\bar{p}$, and the corresponding average gas deviation factor $\bar{Z}$ of natural gas. Then using the proposed reserve evaluation method, by substituting these production performance data of the shale gas reservoir as well as the formation and fluid properties in Table 1

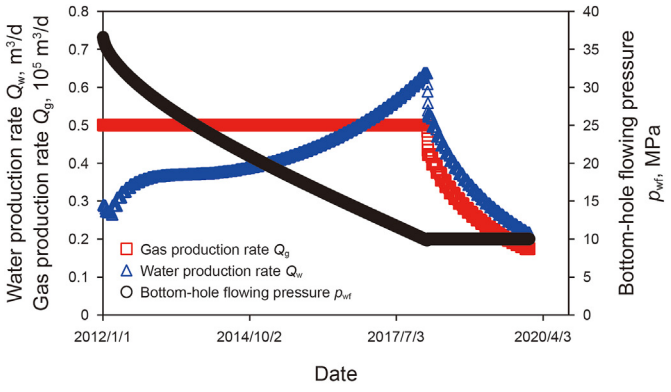

(a) Production performance of one well

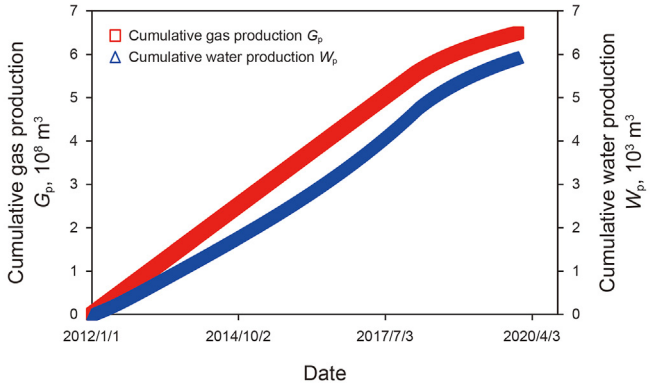

(b) G_p and W_p of the shale gas reservoir

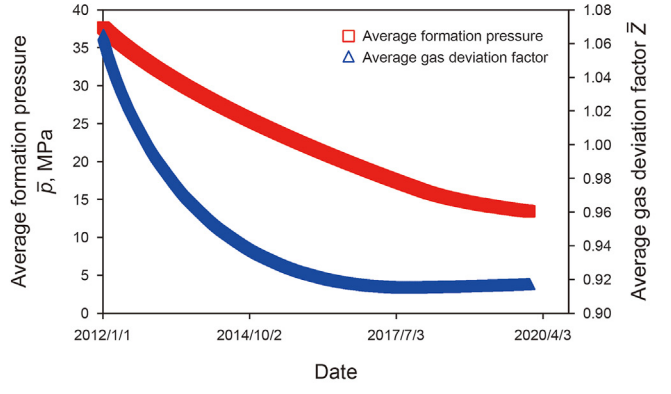

(c) $\bar{p}$ and $\bar{Z}$ of the shale gas reservoir

Fig. 3. Production performance data of the shale gas reservoir.

Table 2
Production performance and the calculated X and Y for the shale gas reservoir.

Date	$\bar{p}$, MPa	$\bar{Z}$	W_p, 10^8 m^3	G_p, 10^8 m^3	X	Y, 10^8 m^3
2012/1/1	37.69	1.065	0	0	−9.002607	0
2013/1/1	32.27	0.993	5.9963E-06	0.915000	−7.952078	0.916562
2014/1/1	28.16	0.955	1.2755E-05	1.827500	−6.907118	1.830513
2015/1/1	24.66	0.934	1.9754E-05	2.740000	−5.864674	2.744183
2016/1/1	21.56	0.922	2.7398E-05	3.652500	−4.826026	3.657638
2017/1/1	18.73	0.916	3.6153E-05	4.567500	−3.790030	4.573427
2018/1/1	16.15	0.915	4.6546E-05	5.480000	−2.765255	5.486586
2019/1/1	14.44	0.916	5.4469E-05	6.108567	−2.044434	6.115452
2020/1/1	13.42	0.917	5.9285E-05	6.490540	−1.595077	6.497496

into Eqs. (11) and (12), the Y and X corresponding to each date can be calculated, respectively, as shown in the last two columns of Table 2. The scatter plot of Y versus X and the linear fitting result for this shale gas reservoir are shown in Fig. 4. It can be seen that a straight-line relationship can perfectly fit all the scatter points with R^2 of nearly 1, indicating the proposed reserve evaluation method is reasonable and effective. From this straight line, its slope m is determined to be 0.8790577 (10^8 m^3), and its y-intercept b is determined to be 7.906368 (10^8 m^3).

Substituting the slope m into Eq. (16), the OAGIP of the shale gas reservoir can be calculated to be 7.147251 (10^8 m^3). The value of y-intercept b will be the OFGIP of this shale gas reservoir, which is 7.906368 (10^8 m^3). Since the dissolution coefficient c_s of natural gas in water is 0 for this case, the ODGIP of the shale gas reservoir is 0. Finally, the OGIP of the shale gas reservoir is calculated to be 15.053629 (10^8 m^3) using Eq. (18). Table 3 listed the reservoir volume and reserves output from the simulation model and those evaluated by the proposed reserve evaluation method. Through comparison between the actual reserves from the CMG model and reserves evaluated by the proposed method for this shale gas reservoir, the relative errors for reserves are all within 1%, i.e., the accuracy of the proposed reserve evaluation method is higher than 99% for this case. The straight-line relationship and the accuracy of the evaluated reserves demonstrate that the proposed reserve evaluation method for shale gas reservoir is rational, accurate, and effective.

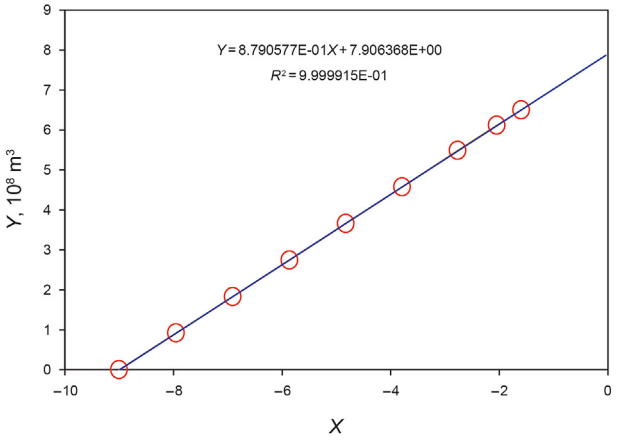

Fig. 4. The scatter plot of Y versus X and the linear fitting result for the shale gas reservoir.

Table 3
Reserve calculation results and error analyses for the shale gas reservoir.

Parameter	Value, 10^8 m^3		Relative error, %
	CMG model	The proposed method	
Reservoir volume Ah	0.87348551	0.87905770	0.634
OFGIP	7.86364717	7.90636800	0.540
OAGIP	7.09712062	7.14725135	0.701
ODGIP	0	0	/
OGIP	14.96076779	15.05361935	0.617

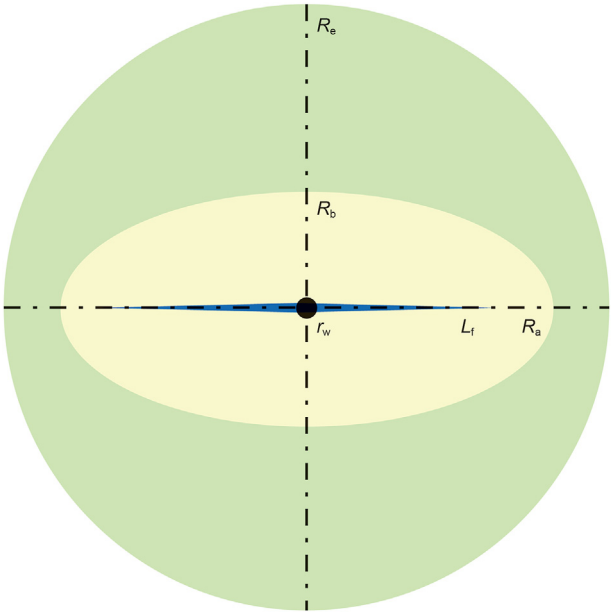

Fig. 5. Physical model of a vertically fractured CBM well using CBMDPA.

3.2. Validation for CBM reservoir

In order to consider the effect of dissolved gas on reserve evaluation, the coalbed methane dynamic performance analysis software (CBMDPA) is applied to validate the proposed reserve evaluation method for CBM reservoir, which can consider the dissolve gas and has been proved to be accurate and applicable (Shi et al., 2018a, 2018b, 2019a, 2019b, 2020, 2021a, 2021b). The physical model of a vertically fractured CBM well using CBMDPA is shown in Fig. 5. This numerical simulation model is a cylinder with the drainage radius R_e of 150 m, fracture half-length L_f of 70 m, thickness of the reservoir h of 10 m, reservoir volume Ah of 0.007068583 (10^8 m^3). The single porosity model with gas and water two phase flow is also used in CBMDPA. The formation and fluid properties of

Table 4
Formation and fluid properties of the CBM reservoir.

Parameter	Value
Bulk density of rock ρ_B, t/m^3	1.5
Langmuir volume V_L, m^3/t	10
Langmuir pressure p_L, MPa	2
Critical desorption pressure p_d, MPa	4.5
Initial pressure p_i, MPa	7.2
Initial porosity ϕ_i	0.0399
Initial water saturation S_{wi}	0.95
Pore volume compressibility c_p, MPa^{-1}	0.00252187
Water compressibility c_w, MPa^{-1}	0.000435
Water volume factor B_w, m^3/sm^3	1
Specific gravity of natural gas γ_g	0.552
Formation temperature T, K	299
Henry constant H, MPa	4180
Poisson's ratio ν	0.3
Maximum strain under matrix shrinkage effect ε_{max}	0.035

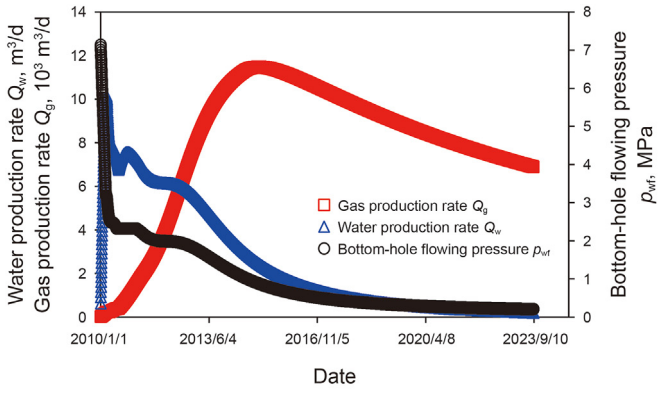

(a) Production performance of the CBM well

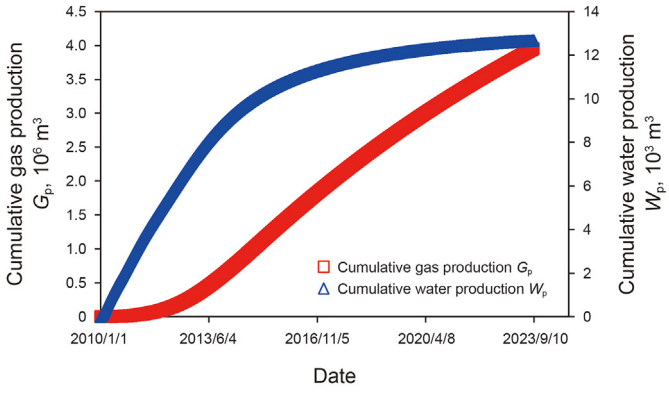

(b) G_p and W_p of the CBM reservoir

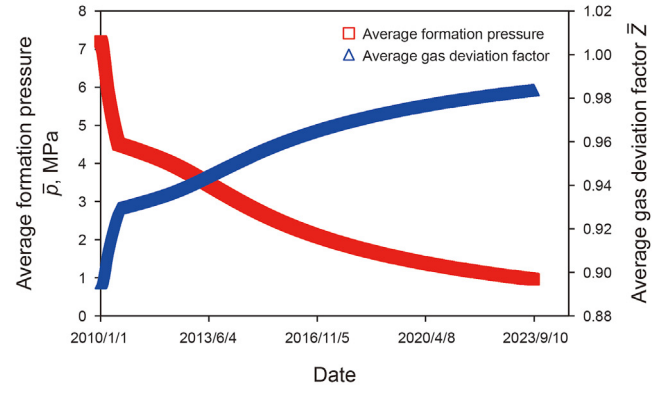

(c) $\bar{p}$ and $\bar{Z}$ of the CBM reservoir

Fig. 6. Production performance data of the CBM reservoir.

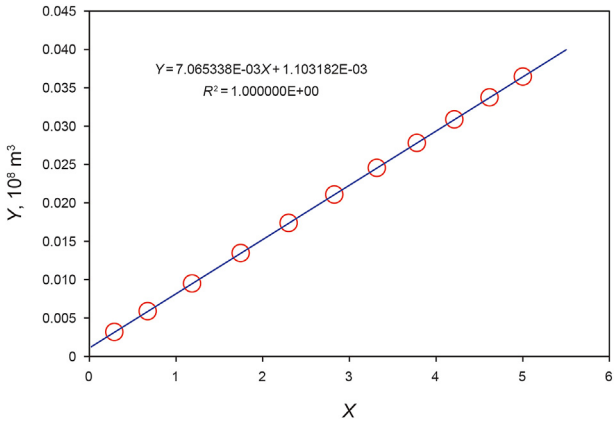

Fig. 7. The scatter plot of Y versus X and the linear fitting result for the CBM well.

this model are shown in Table 4. For this model, OFGIP is 0.00110087 (10^8 m^3), OAGIP is 0.07340452 (10^8 m^3), ODGIP is 0.00057433 (10^8 m^3) and OGIP is 0.07507971 (10^8 m^3).

Production performance of this CBM well is shown in Fig. 6a. As shown in Fig. 6a, the well is produced according to the designed bottom-hole flowing pressure, and the daily gas production increases gradually, with a peak value of 1135 m^3/d, and then decreases slowly. The dynamics of cumulative gas production G_p and cumulative water production W_p with producing time are shown in Fig. 6b. The average formation pressure $\bar{p}$ and the corresponding average deviation factor $\bar{Z}$ are shown in Fig. 6c. Water influx is not considered in this case, so W_e is 0. By substituting the values of Poisson's ratio ν and maximum strain under matrix shrinkage effect ε_{max} in Table 4 into Eq. (3), the matrix shrinkage coefficient c_a is calculated to be 0.013125. By substituting Henry's constant H in Table 4 into Eq. (4), the dissolution coefficient of natural gas in water c_s is calculated to be 0.297713982 MPa^{-1}.

The annual production performance data of this CBM well are listed in Table 5, including date, cumulative water production W_p, cumulative gas production G_p, average formation pressure $\bar{p}$, and the corresponding average gas deviation coefficient $\bar{Z}$ of natural gas. Then using the proposed reserve evaluation method, by substituting these production performance data of the CBM well as well as the formation and fluid properties in Table 4 into Eqs. (11) and (12), the Y and X corresponding to each date can be calculated, respectively, as shown in the last two columns of Table 5. The scatter plot of Y versus X and the linear fitting result for this CBM well are shown in Fig. 7. It can be seen that a straight-line relationship can perfectly fit all the scatter points with R^2 of 1, indicating the proposed reserve evaluation method is reasonable and effective for CBM reservoirs. From this straight line, its slope m is determined to be 0.007065338 (10^8 m^3), and its y-intercept b is determined to be

Table 5
Production performance and the calculated X and Y for the CBM well.

Date	$\bar{p}$, MPa	$\bar{Z}$	W_p, 10^8 m^3	G_p, 10^8 m^3	X	Y, 10^8 m^3
2010/1/1	4.07	0.935	5.1348E-05	0.00104118	0.289370	3.148983E-03
2011/1/1	3.65	0.941	7.3147E-05	0.00318800	0.673123	5.860689E-03
2012/1/1	3.16	0.948	9.0076E-05	0.00663855	1.184437	9.472279E-03
2013/1/1	2.72	0.955	1.0125E-04	0.01071755	1.745437	1.343460E-02
2014/1/1	2.34	0.961	1.0860E-04	0.01485232	2.300119	1.735249E-02
2015/1/1	2.04	0.965	1.1368E-04	0.01879756	2.825676	2.106539E-02
2016/1/1	1.79	0.969	1.1734E-04	0.02248989	3.317156	2.453815E-02
2017/1/1	1.59	0.973	1.2008E-04	0.02594609	3.777924	2.779439E-02
2018/1/1	1.41	0.976	1.2218E-04	0.02918319	4.210525	3.085194E-02
2019/1/1	1.26	0.978	1.2382E-04	0.03222832	4.618549	3.373608E-02
2020/1/1	1.13	0.980	1.2510E-04	0.03508314	5.002076	3.644728E-02

Table 6
Reserve calculation results and error analyses for the CBM reservoir.

Parameter	Value, 10^8 m^3		Relative error, %
	CBMDPA model	The proposed model	
Reservoir volume *Ah*	0.00706858	0.00706534	0.046
OFGIP	0.00110087	0.00110318	0.210
OAGIP	0.07340452	0.07337082	0.046
ODGIP	0.00057433	0.00057407	0.045
OGIP	0.07507971	0.07504807	0.042

Table 7
Formation and fluid properties of Fuling shale gas field.

Parameter	Value
Bulk density of rock ρ_B, t/m^3	2.47
Langmuir volume V_L, m^3/t	2.76
Langmuir pressure p_L, MPa	3.69
Critical desorption pressure p_d, MPa	24.138
Initial pressure p_i, MPa	24.138
Initial porosity ϕ_i	0.021
Initial water saturation S_{wi}	0.2
Pore volume compressibility c_p, MPa^{-1}	0.0087
Water compressibility c_w, MPa^{-1}	0.000435
Water volume factor B_w, m^3/sm^3	1
Specific gravity of natural gas γ_g	0.69
Formation temperature *T*, K	366.48
Henry constant *H*, MPa	7040
Matrix shrinkage coefficient c_a	0

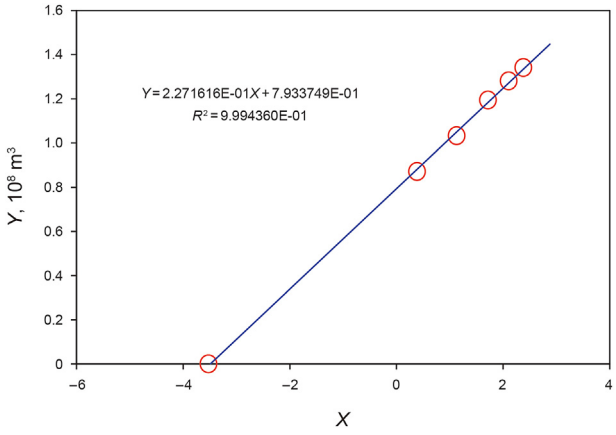

Fig. 8. The scatter plot of *Y* versus *X* and the linear fitting result for Fuling shale gas field.

0.00110318 (10^8 m^3).

Substituting the slope *m* into Eq. (16), the OAGIP controlled by this CBM well can be calculated to be 0.07337082 (10^8 m^3). The value of *y*-intercept *b* will be the OFGIP controlled by this CBM well, which is 0.00110318 (10^8 m^3). Substituting the slope *m* into Eq. (17), the OAGIP controlled by this CBM well is calculated to be 0.00057407 (10^8 m^3). Finally, the OGIP controlled by this CBM well is calculated to be 0.07504807 (10^8 m^3) using Eq. (18). Table 6 listed the reservoir volume and reserves output form CBMDPA model and those evaluated by the proposed reserve evaluation method. Through comparisons between the actual reserves and evaluated reserves controlled by this CBM well, the relative errors for reserves are all within 0.5%, i.e., the accuracy of the proposed reserve evaluation method is higher than 99.5% for this case. The straight-line relationship and the accuracy of the evaluated reserves demonstrate that the proposed reserve method for CBM reservoirs is rational, accurate, and effective.

4. Field applications

4.1. Application in Fuling shale gas field

The Fuling shale gas field is located in Fuling District, Chongqing, Southwest China. From the perspective of geological structure, it is located in the Eastern edge of Sichuan Basin. In this work, part of the shale gas field which is controlled by a horizontal well group is selected as the application area for reserve calculation (Zhang et al., 2013). The static properties of this block are shown in Table 7, and the dynamic production data of the horizontal well group in the Fuling gas field are shown in first five columns of Table 8. The data of average reservoir pressure $\overline{p}$ is from the interpretation results of pressure build-up test in field. There is no water influx in the Fuling shale gas field, so W_e is constantly equal to 0. The matrix shrinkage coefficient c_a is equal to 0. Substituting the value of Henry's constant *H* in Table 7 into Eq. (4) gives the dissolution coefficient of natural gas in water c_s, which is equal to 0.1767677 MPa^{-1}.

By substituting the dynamic performance data of this well group in the Fuling gas field in Table 8 and the formation and fluid properties in Table 7 into Eqs. (11) and (12), the *Y* and *X* corresponding to each date can be calculated, as shown in the last two columns of Table 8. A scatter plot of *Y* versus *X* is drawn and the scatter points with linear equation is fitted, as shown in Fig. 8. The high R^2 of this fitting straight line, which is 0.9994, indicates that the proposed reserve evaluation is reasonable. From this straight-line relationship, the slope *m* is determined to be 0.2271616 (10^8 m^3) and the *y*-intercept *b* is determined to be 0.7933749 (10^8 m^3). Then, by substituting the slope *m* into Eq. (15), the OFGIP is calculated to be 0.79845046 (10^8 m^3), which is nearly consistent with that evaluated using the *y*-intercept, indicating that there is no

Table 8
Production performance and the calculated *X* and *Y* for Fuling shale gas field.

Date	$\overline{p}$, MPa	$\overline{Z}$	W_p, 10^8 m^3	G_p, 10^8 m^3	*X*	*Y*, 10^8 m^3
2014/9/15	24.138	0.8956	0	0	−3.520395	0
2016/6/2	7.807	0.9208	0	0.87	0.387325365	0.87
2016/9/21	5.759	0.9376	0	1.032	1.13154949	1.032
2017/1/7	4.455	0.9498	0	1.193	1.718870219	1.193
2017/5/11	3.731	0.9571	0	1.28	2.105881142	1.28
2017/8/18	3.276	0.9618	0	1.34	2.379727175	1.34

Table 9
Reserve calculation results for the well group in Fuling shale gas field.

Parameter	Evaluated value, 10^8 m^3			
	King (1990)	Williams-Kovacs et al. (2012)	Zhang et al. (2013)	The proposed method
Reservoir volume *Ah*	/	/	/	0.2271616
OFGIP	/	/	/	0.79845046
OAGIP	/	/	/	1.34326050
ODGIP	/	/	/	0.00407088
OGIP	2.071	2.245	2.18	2.14578184

Table 10
The formation and fluid properties of Baode CBM field.

Parameter	Value
Bulk density of rock ρ_B, t/m^3	1.58
Langmuir volume V_L, m^3/t	10.79
Langmuir pressure p_L, MPa	2.12
Critical desorption pressure p_d, MPa	6.08
Initial pressure p_i, MPa	6.9
Initial porosity ϕ_i	0.09
Initial water saturation S_{wi}	0.9475
Pore volume compressibility c_p, MPa^{-1}	0.001087
Water compressibility c_w, MPa^{-1}	0.00047
Water volume factor B_w, m^3/sm^3	1.008
Specific gravity of natural gas γ_g	0.608
Formation temperature *T*, K	301.15
Henry constant *H*, MPa	4402
Poisson's ratio ν	0.3
Maximum strain under matrix shrinkage effect ε_{max}	0.035

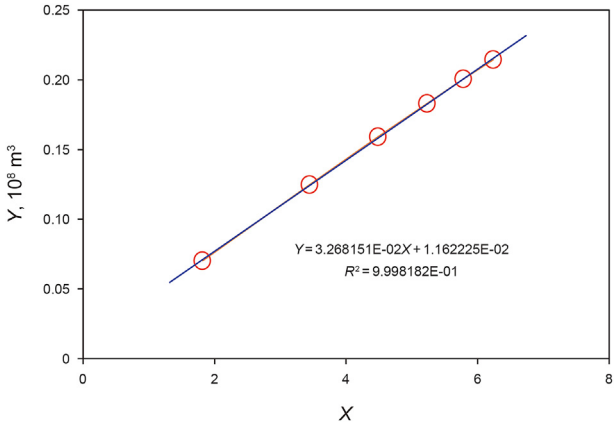

Fig. 9. The scatter plot of *Y* versu *X* and the linear fitting result for Baode CBM reservoir.

need to adjust the initial water saturation. Finally, according to Eqs. (15)–(18), the OFGIP, OAGIP, ODGIP, and OGIP are calculated to be 0.79845046 (10^8 m^3), 1.34326050 (10^8 m^3), 0.00407088 (10^8 m^3), and 2.14578184 (10^8 m^3), respectively. Table 9 shows the reserve calculation results using different methods for this well group in the Fuling shale gas field. Except the proposed reserve evaluation method can determine the OAGIP, OFGIP, ODGIP, and OGIP, other methods only can estimate the OGIP. If using the proposed reserve evaluation method, more detailed information about reserves of shale gas reservoir can be clarified, and only the straight-line fitting approach is used to determine all kinds of reserves without iteration, proving that the proposed method has great advantages compared with other current methods.

From the determined reserves in Table 9, it can be easily calculated that the free gas, adsorbed gas, and dissolved gas account for 37.21%, 62.60%, and 0.19% of the total gas for this well group in the Fuling shale gas field, respectively. For this well group in the Fuling shale gas field, the free gas content is less than the adsorbed gas content, which is different from the common knowledge of larger free gas content in the Fuling shale gas field. The reason may come from the difference between the porosity values. The lower porosity yields the lower free gas content, but the porosity almost does not affect adsorbed gas content. The porosity of shale formation for this well group in the Fuling shale gas field, which is only 2.1%, is less than the average porosity for the whole Fuling shale gas field, which is 4.61% (Fang and Meng, 2020). Other researchers, such as Liu et al. (2021) and Bao et al. (2022), also concluded that the porosity of shale formation in the Fuling shale gas field ranges from 1.77% to 5.54% and from 3.38% to 7.8%, respectively. Maybe the study blocks are different, but all these knowledges about the porosity of shale formation in the Fuling shale gas field prove the shale formation with the porosity of 2.1% for this case is in a low porosity area.

4.2. Application in Baode CBM field

Baode CBM field is located in the eastern edge of Ordos Basin and northwest Shanxi province. The administrative division is subordinate to Baode county, Xinzhou city, Shanxi province. In this work, part of the CBM field which are controlled by a group of fractured vertical wells is selected as the application area for reserve calculation (Zhang et al., 2013). The static properties of this block are shown in Table 10, and the dynamic production data are

Table 11
Production performance and the calculated *X* and *Y* for Baode CBM field.

Date	$\bar{p}$, MPa	$\bar{Z}$	W_p, 10^8 m^3	G_p, 10^8 m^3	*X*	*Y*, 10^8 m^3
2015/1/1	6.9	0.8843	0	0	−0.753936	0.000000
2015/11/2	3.61	0.9358	0.00006106	0.068	1.815430375	0.070225562
2016/8/23	2.48	0.9552	0.00008264	0.1227	3.446880597	0.124726059
2017/6/22	1.96	0.9644	0.00009541	0.1573	4.484526789	0.159130529
2018/4/19	1.65	0.9699	0.00010441	0.1813	5.234182896	0.182976528
2019/2/13	1.45	0.9735	0.00011134	0.1991	5.784846662	0.200665121
2019/12/9	1.3	0.9762	0.00011697	0.2131	6.239013839	0.214569969

Table 12
Reserve calculation results for the well group in Baode CBM field.

Parameters	Evaluated value, 10^8 m^3		
	Chen and Hu (2008)	Zhang et al. (2013)	The proposed method
Reservoir volume *Ah*	/	/	0.03268151
OFGIP	0.01051	0.03434	0.01161286
OAGIP	0.41787	0.38501	0.41311444
ODGIP	/	/	0.00543624
OGIP	0.42838	0.41935	0.43016353

shown in first five columns of Table 11. The data of average reservoir pressure $\overline{p}$ is from the interpretation results of pressure build-up test in field. Baode CBM field has no edge water and bottom water, so W_e is 0. By substituting the values of Poisson's ratio ν and maximum strain under matrix shrinkage effect ε_{max} in Table 10 into Eq. (3), the matrix shrinkage coefficient c_a is calculated to be 0.013125. By substituting Henry's constant H in Table 10 into Eq. (4), the dissolution coefficient of natural gas in water c_s is calculated to be 0.28269978 MPa^{-1}.

By substituting the dynamic performance data of this well group in Baode CBM field in Table 11 and the formation properties in Table 10 into Eq. (11) and Eq. (12), the Y and X corresponding to each date can be calculated, as shown in the last two columns of Table 11. Draw a scatter plot of Y versus X and fit the scatter points with linear equation, as shown in Fig. 9. The high R^2 of this fitting straight line, which is 0.9998, indicates that the proposed reserve evaluation is reasonable. From this straight-line relationship, the slope m is determined to be 0.03268151 (10^8 m^3) and the y-intercept b is determined to be 0.01162225 (10^8 m^3). Through adjusting the value of the initial water saturation, when it is equal to 0.9475, the OFGIP evaluated using the slope and that evaluated using the y-intercept are consistent. Finally, according to Eqs. (15)–(18), the OFGIP, OAGIP, ODGIP, and OGIP are calculated to be 0.01161286 (10^8 m^3), 0.41311444 (10^8 m^3), 0.00543624 (10^8 m^3), and 0.43016353 (10^8 m^3), respectively. Table 12 shows the reserve calculation results using different methods for this well group in the Baode CBM field. As shown in Table 12, all the reserves, including OFGIP, OAGIP, ODGIP, and OGIP, can be determined by using the proposed reserve evaluation method, while, other methods fail to estimate the ODGIP. If using the proposed reserve evaluation method, more detailed information about reserves of CBM reservoirs can be clarified, and only the straight-line fitting approach is used to determine all kinds of reserves without iteration, proving that the proposed method has great advantages compared with other current methods.

5. Conclusions

The generalized material balance equation (GMBE) and the corresponding straight-line fitting method for estimating reserves of free gas, adsorbed gas, and dissolved gas for shale gas and CBM reservoirs is established, in which the effects of critical desorption pressure, stress sensitivity, matrix shrinkage, water production, water influx, and dissolution of natural gas in water are considered. Then, validations of the method for shale gas reservoirs and CBM reservoirs using CMG-IMEX and CBMDPA are conducted. Finally, field applications in the Fuling shale gas field and the Baode CBM field are presented. From this work, the following conclusions can be obtained:

(1) For adsorptive gas reservoirs, including shale gas reservoirs and CBM reservoirs, a linear relationship can be obtained through transforming the GMBE, using the slope and y-intercept of this straight line, the reservoir volume, OFGIP, OAGIP, ODGIP, and OGIP can be calculated easily.
(2) Two validation cases prove that the GMBE and the corresponding straight-line reserve evaluation method is rational, accurate, and effective for both shale gas reservoirs and CBM reservoirs.
(3) Two application cases demonstrate that the proposed reserve evaluation method can interpret more detailed information about reserves of shale gas and CBM reservoirs, and only the straight-line fitting approach is used to determine all kinds of reserves without iteration, proving that the proposed method has great advantages compared with other current methods.

Acknowledgments

The research was supported by Science and Technology Major Project of Shanxi Province, China (No. 20201101002). The authors acknowledge National Science and Technology Major Project of China, China (No. 2016ZX05043002), National Natural Science Foundation Project of China, China (No. 51874319), and Science Foundation of China University of Petroleum (Beijing), China (No. 2462020QNXZ003) to support part of this work. The authors also thank Computer Modelling Group for giving us the authorization to use CMG-IMEX software.

References

Ahmed, T., Centilmen, A., Roux, B., 2006. A generalized material balance equation for coalbed methane reservoirs. In: SPE Annual Technical Conference and Exhibition. https://doi.org/10.2118/102638-MS.
Akkutlu, I., Efendiev, Y., Savatorova, V., 2015. Multi-scale asymptotic analysis of gas transport in shale matrix. Transport Porous Media 107, 235–260. https://doi.org/10.1007/s11242-014-0435-z.
Bao, H., Liang, B., Zheng, A., Xiao, J., Liu, C., Liu, L., 2022. Application of geology and engineering integration in stereoscopic exploration and development of Fuling shale gas demonstration area. China Petroleum Exploration 27 (1), 88–98 (in Chinese).
Chen, Y., Hu, J., 2008. Derivation of methods for estimating OGIP and recoverable reserves and recovery ratio of saturated coal-seam gas reservoirs. Oil Gas Geol. 29 (1), 151–156 (in Chinese).
Clarkson, C., McGovern, J., 2001. Study of the potential impact of matrix free gas storage upon coalbed gas reserves and production using a new material balance equation. International Coalbed Methane Symposium.
Clarkson, C., Pan, Z., Palmer, I., Harpalani, S., 2010. Predicting sorption-induced strain and permeability increase with depletion for coalbed-methane reservoirs. SPE J. 15 (1), 152–159. https://doi.org/10.2118/114778-PA.
Dranchuk, P., Abou-Kassem, H., 1975. Calculation of Z factors for natural gases using equations of state. J. Can. Petrol. Technol. 14 (3), 34–36. https://doi.org/10.2118/75-03-03.
Fang, D., Meng, Z., 2020. Main controlling factors of shale gas enrichment and high yield: a case study of Wufeng-Longmaxi formations in Fuling area, Sichuan Basin. Petroleum Geology & Experiment 42 (1), 37–41 (in Chinese).
Fuentes-Cruz, G., Vasquez-Cruz, M., 2022. Reservoir performance analysis through the material balance equation: an integrated review based on field examples. J. Petrol. Sci. Eng. 208, 109377. https://doi.org/10.1016/j.petrol.2021.109377.
Harpalani, S., Schraufnagel, R., 1990. Shrinkage of coal matrix with release of gas and its impact on permeability of coal. Fuel 69 (5), 551–556. https://doi.org/10.1016/0016-2361(90)90137-F.
Ibrahim, A., Nasr-El-Din, H., 2015. A comprehensive model to history match and predict gas/water production from coal seams. Int. J. Coal Geol. 146, 79–90. https://doi.org/10.1016/j.coal.2015.05.004.
Jensen, D., Smith, L., 1997. A practical approach to coalbed methane reserve

prediction using a modified material balance technique. International Coalbed Methane Symposium.
Kazemi, N., Ghaedi, M., 2020. Production data analysis of gas reservoirs with edge aquifer drive: a semi-analytical approach. J. Nat. Gas Sci. Eng. 80, 103382. https://doi.org/10.1016/j.jngse.2020.103382.
King, G., 1990. Material balance techniques for coal seam and Devonian shale gas reservoirs. In: SPE Annual Technical Conference and Exhibition. https://doi.org/10.2118/20730-MS.
King, G., 1993. Material-balance techniques for coal-seam and Devonian shale gas reservoirs with limited water influx. SPE Reservoir Eng. 8, 67–72. https://doi.org/10.2118/20730-PA.
Li, J., Li, X., Wang, X., Li, Y., Shi, J., Feng, D., Bai, Y., Xu, M., 2016. A quantitative model to determine water-saturation distribution characteristics inside shale inorganic pores. Acta Pet. Sin. 37 (7), 903–913 (in Chinese).
Li, J., Zhang, T., Li, Y., Liang, X., Wang, X., Zhang, J., Zhang, Z., Shu, H., Rao, D., 2020. Geochemical characteristics and genetic mechanism of the high-N_2 shale gas reservoir in the Longmaxi Formation, Dianqianbei Area, China. Petrol. Sci. 17, 939–953. https://doi.org/10.1007/s12182-020-00456-8.
Liu, J., Xie, L., He, B., Zhao, P., Ding, H., 2021. Performance of free gases during the recovery enhancement of shale gas by CO_2 injection: a case study on the depleted Wufeng–Longmaxi shale in northeastern Sichuan Basin, China. Petrol. Sci. 18, 530–545. https://doi.org/10.1007/s12182-020-00533-y.
Liu, S., Harpalani, S., 2013. Permeability prediction of coalbed methane reservoirs during primary depletion. Int. J. Coal Geol. 113 (3), 1–10. https://doi.org/10.1016/j.coal.2013.03.010.
Miao, Y., Zhao, C., Zhou, G., 2020. New rate-decline forecast approach for low-permeability gas reservoirs with hydraulic fracturing treatments. J. Petrol. Sci. Eng. 190, 107112. https://doi.org/10.1016/j.petrol.2020.107112.
Miao, Y., Zhao, C., Zhou, G., 2022. Gas flowrate evaluation in coal coupling the matrix shrinkage effect caused by water extraction. J. Energy Resour. Technol. 144, 4051301. https://doi.org/10.1115/1.4051301.
Moghadam, S., Jeje, O., Mattar, L., 2011. Advanced gas material balance in simplified format. J. Can. Petrol. Technol. 50, 90–98. https://doi.org/10.2118/139428-PA.
Moghadam, S., Jeje, O., Mattar, L., 2009. Advanced gas material balance, in simplified format. In: Canadian International Petroleum Conference. https://doi.org/10.2118/2009-149.
Nie, H., Chen, Q., Zhang, G., Sun, C., Wang, P., Lu, Z., 2021. An overview of the characteristic of typical WufengeLongmaxi shale gas fields in the Sichuan Basin, China. Nat. Gas. Ind. B 8, 217–230. https://doi.org/10.1016/j.ngib.2021.04.001.
Orozco, D., Aguilera, R., 2017. Material-balance equation for stress-sensitive shale-gas-condensate reservoirs. SPE Reservoir Eval. Eng. 20, 197–214. https://doi.org/10.2118/177260-PA.
Orozco, D., Aguilera, R., 2018. Use of dynamic data and a new material-balance equation for estimating average reservoir pressure, original gas in place, and optimal well spacing in shale gas reservoirs. SPE Reservoir Eval. Eng. 21, 1035–1044. https://doi.org/10.2118/185598-PA.
Palmer, I., 2009. Permeability changes in coal: analytical modeling. Int. J. Coal Geol. 77 (1), 119–126. https://doi.org/10.1016/j.coal.2008.09.006.
Pan, X., Zhang, G., Chen, J., 2020. The construction of shale rock physics model and brittleness prediction for high-porosity shale gas-bearing reservoir. Petrol. Sci. 17 (3), 658–670. https://doi.org/10.1007/s12182-020-00432-2.
Seidle, J., 1999. A modified p/Z method for coal wells. In: SPE Rocky Mountain Regional Meeting. https://doi.org/10.2118/55605-MS.
Shi, J., Durucan, S., 2005. A model for changes in coalbed permeability during primary and enhanced methane recovery. SPE Reservoir Eval. Eng. 8 (4), 291–299. https://doi.org/10.2118/87230-PA.
Shi, J., Chang, Y., Wu, S., Xiong, X., Liu, C., Feng, K., 2018a. Development of material balance equations for coalbed methane reservoirs considering dewatering process, gas solubility, pore compressibility and matrix shrinkage. Int. J. Coal Geol. 195, 200–216. https://doi.org/10.1016/j.coal.2018.06.010.
Shi, J., Wang, S., Zhang, H., Sun, Z., Hou, C., Chang, Y., Xu, Z., 2018b. A novel method for formation evaluation of undersaturated coalbed methane reservoirs using dewatering data. Fuel 229, 44–52. https://doi.org/10.1016/j.fuel.2018.04.144.
Shi, J., Hou, C., Wang, S., Xiong, X., Wu, S., Liu, C., 2019a. The semi-analytical productivity equations for vertically fractured coalbed methane wells considering pressure propagation process, variable mass flow, and fracture conductivity decrease. J. Petrol. Sci. Eng. 178, 528–543. https://doi.org/10.1016/j.petrol.2019.03.047.
Shi, J., Wang, S., Wang, K., Liu, C., Wu, S., Sepehrnoori, K., 2019b. An accurate method for permeability evaluation of undersaturated coalbed methane reservoirs using early dewatering data. Int. J. Coal Geol. 202, 147–160. https://doi.org/10.1016/j.coal.2018.12.008.
Shi, J., Wu, J., Sun, Z., Xiao, Z., Liu, C., Sepehrnoori, K., 2020. Methods for simultaneously evaluating reserve and permeability of undersaturated coalbed methane reservoirs using production data during the dewatering stage. Petrol. Sci. 17, 1067–1086. https://doi.org/10.1007/s12182-019-00410-3.
Shi, J., Jia, Y., Wu, J., Xu, F., Sun, Z., Liu, C., Meng, Y., Xiong, X., Liu, C., 2021a. Dynamic performance prediction of coalbed methane wells under the control of bottomhole pressure and casing pressure. J. Petrol. Sci. Eng. 196, 107799. https://doi.org/10.1016/j.petrol.2020.107799.
Shi, J., Wu, J., Fang, Y., Lu, J., Hou, C., Li, X., Zhang, S., Xiong, X., 2021b. A new coal reservoir permeability model considering the influence of pulverized coal blockage and its application. Nat. Gas. Ind. B 8 (1), 67–78. https://doi.org/10.1016/j.ngib.2020.06.004.
Shi, J., Wu, J., Lv, M., Li, Q., Liu, C., Zhang, T., Sun, Z., He, M., Li, X., 2021c. A new straight-line reserve evaluation method for water bearing gas reservoirs with high water production rate. J. Petrol. Sci. Eng. 196, 107808. https://doi.org/10.1016/j.petrol.2020.107808.
Sun, Z., Huang, B., Li, Y., Lin, H., Shi, S., Yu, W., 2021. Nanoconfined methane flow behavior through realistic organic shale matrix under displacement pressure: a molecular simulation investigation. J. Pet. Explor. Prod. Technol. https://doi.org/10.1007/s13202-021-01382-0.
Wang, T., Tian, S., Liu, Q., Li, G., Sheng, M., Ren, W., Zhang, P., 2021. Pore structure characterization and its effect on methane adsorption in shale kerogen. Petrol. Sci. 18 (2), 565–578. https://doi.org/10.1007/s12182-020-00528-9.
Williams-Kovacs, J., Clarkson, C., Nobakht, M., 2012. Impact of material balance equation selection on rate-transient analysis of shale gas. In: SPE Annual Technical Conference and Exhibition. https://doi.org/10.2118/158041-MS.
Yang, X., Lei, Y., Zhang, J., Chen, S., Chen, L., Zhong, K., He, L., Li, D., Wu, Q., 2021. Depositional environment of shales and enrichment of organic matters of the lower cambrian niutitang formation in the upper yangtze region. Nat. Gas. Ind. B 8, 666–679. https://doi.org/10.1016/j.ngib.2021.11.001.
Zhang, L., Chen, G., Zhao, Y., Liu, Q., Zhang, H., 2013. A modified material balance equation for shale gas reservoirs and a calculation method of shale gas reserves. Nat. Gas. Ind. 33, 66–70 (in Chinese).
Zhang, X., Feng, Q., Wang, X., Du, P., 2013. Establishment and application of material balance equations for low-rank coalbed methane reservoirs. Nat. Gas Geosci. 24, 1311–1315 (in Chinese).
Zhou, Q., Tian, H., Chen, G., Xu, Q., 2013. Geological model of dissolved gas in pore water of gas shale and its controlling factors. J. China Coal Soc. 38, 800–804 (in Chinese).
Zhu, Q., Yang, Y., Zuo, Y., Song, Y., Guo, W., Tang, F., Ren, J., Wang, G., 2020. On the scientific exploitation of high-rank CBM resources. Nat. Gas. Ind. B 7 (4), 403–409. https://doi.org/10.1016/j.ngib.2020.01.008.